CrossMark

RESEARCH PAPER

Size-dependent production of radicals in catalyzed reduction of Eosin Y using gold nanorods

Guojun Weng · Ying Qi · Jianjun Li ·
Junwu Zhao

Abstract Gold nanostructures have been widely used as catalysts for chemical processes, energy conversion, and pollution control. The size of gold nanocatalysts is thus paramount for their catalytic activity. In this paper, gold nanorods with different sizes were prepared by means of the improved seeding growth approach by adding aromatic additive. The sizes and aspect ratios of the obtained gold nanorods were calculated according to the TEM characterization. Then, we studied the catalytic activities of gold nanorods using a model reaction based on the reduction of Eosin Y by $NaBH_4$. By monitoring the absorption intensities of the radicals induced by gold nanorods in real time, we observed the clear size-dependent activity in the conversion of EY^{2-} to EY^{3-}. The conversion efficiency indicated that the gold nanorods with the smallest size were catalytically the most active probably due to their high number of coordinatively unsaturated surface atoms. In addition, a compensation effect dominated by the surface area of nanorods was observed in this catalytic reduction, which could be primarily attributed to the configuration of Eosin Y absorbed onto the surfaces of gold nanorods.

G. Weng · Y. Qi · J. Li · J. Zhao (✉)
The Key Laboratory of Biomedical Information
Engineering of Ministry of Education, School of Life
Science and Technology, Xi'an Jiaotong University, No.
28 Xianning West Road, Xi'an 710049, China
e-mail: nanoptzhao@163.com

Introduction

Gold nanoparticles are already being used in a range of applications, including the sensing and diagnostic areas (Saha et al. 2012; Wilson 2008), photothermal therapy (Dreaden et al. 2011, 2012), bio-imaging (Sharma et al. 2006), drug delivery (Ghosh et al. 2008; Han et al. 2007), and so on (Arvizo et al. 2010; Giljohann et al. 2010; Sardar et al. 2009; Sperling et al. 2008). However, another aspect of gold nanoparticles, which is particularly fascinating is their applicability in catalysis for chemical processes, energy conversion, and pollution control (Li et al. 2011; Thompson 2007). However, the sizes of most gold nanoparticles employed as catalysts are usually less than 10 nm and may be as small as 1 nm or even less. The catalytic efficiencies of those gold nanoclusters are determined by the surface energy or electronic structure (Zhu et al. 2011). Furthermore, those supported gold nanocatalysts are used mainly for ethyne hydrochlorination and oxidation of alcohols (Hutchings 2005).

More recently, the catalytic effects of gold nanoparticles with different sizes and shapes have been investigated by means of the oxidation reactions (Fenger et al. 2012; Kundu et al. 2009; Mahmoud and El-Sayed 2011; Zeng et al. 2010). For CTAB-

stabilized gold nanospheres, the most efficient size was 13 nm, which had a clear contradiction to previous reports that smaller particles were more active (Fenger et al. 2012). In addition, Kundu et al. (2009) found that the catalytic efficiency was the highest in the presence of gold nanospheres, intermediate with nanoprisms, and the lowest with the nanorods when the numbers of particles were approximately the same. However, gold nanospheres were catalytically less active than the nanocages probably due to their lacking the open morphology and the thin wall (Zeng et al. 2010). For hollow nanoparticles, the catalysis takes place within the cavity, and the catalytic effect is dependent on the confinement and cage effect (Mahmoud et al. 2013). These reports prove that catalytic activity of gold nanoparticles is strongly affected by their size and shape.

Eosin Y (EY) is a fluorescein derivative dye containing two bromine atoms, and has extensive applications in detecting protein (Lin and Wise 2009) and photovoltaic field (Mali et al. 2012; Yoshida et al. 2009). EY can be reduced by sodium borohydride, and its color changes form yellow to colorless. The fading of EY reduction makes it a suitable mode for studying the catalytic property of nanoparticles. Xia et al. (2011) employed hollow copper microspheres as a catalyst to degrade EY; they found that the degradation rate of EY was enhanced by 7.5–15 times by hollow copper microspheres compared with control group. The catalytic effect of gold nanoparticles had been addressed by borohydride reduction of EY in aqueous solution (Sau et al. 2001). The catalytic activity of the gold nanoparticles had a strong relationship with the size regimes of the particles. The rate of EY reduction decreased with the increasing particle size when the diameter is below 15 nm, while it increased with the diameter above 15 nm. Srivastava et al. (2011) employed gold nanorods with an aspect ratio of 10 to catalyze the reduction of EY with sodium borohydride. The rate constant was very large in comparison to that without gold nanorods. Spectro-electrochemical studies showed that the redox reduction of EY by sodium borohydride occurs through two different pathways: two-electron and one-electron reduction (Bannerjee and Negi 1973; Goux et al. 2007; Issa et al. 1973). However, the former research presumed that EY was reduced by sodium borohydride though two-electron pathway, but the details of the reduction process were not investigated.

Our group studied the reduction of EY by sodium borohydride in the presence of gold solid and hollow nanoparticles in detail (Mahmoud and Weng 2013; Weng et al. 2012). We found that gold nanocatalysts could change the number of electrons involved in the reduction reaction of EY. The reduction pathway changed from two-electron reduction to one-electron reduction. EY was reduced by one-electron pathway and formed the radical EY^{3-} during the second stage of the reduction reaction. The conversion ratio of EY to EY^{3-} in the presence of hollow nanospheres was found to be three times higher than that found while using the solid nanospheres. In the present paper, gold nanorods with different sizes are prepared and used to catalyze the reduction reaction of EY by borohydride. It is found that the pathway of reaction of EY is one-electron reduction at the second stage in the presence of gold nanorods of each set. Furthermore, the production of the one-electron-reduced EY^{3-} is found to be dependent on the size of gold nanorods. Gold nanorods with the smallest size are the most efficient for production of the radical EY^{3-}.

Experimental

Chemicals and materials

The following chemicals were purchased and used as received in all experiments. Hexadecyltrimethylammonium bromide (CTAB) ($C_{19}H_{42}BrN$), L-Ascorbic acid ($C_6H_8O_6$), eosin Y ($C_{20}H_8Br_4O_5$), and sodium borohydride ($NaBH_4$) were purchased from Sigma. Hydrogen tetrachloroauratetrihydrate ($HAuCl_4 \cdot 3H_2O$) was obtained from Shanghai Chemical Reagent Co. Ltd. (China). 5-bromosalicylic acid ($C_7H_5BrO_3$) was purchased from TCI China. Silver nitrate ($AgNO_3$) was obtained from Xi'an Hairmer Co.Ltd. (China). The ultrapure water with 18.2 $\Omega M \cdot cm^{-1}$ was used throughout the experiments.

Instrumentation

Absorption spectra of gold nanorods were recorded on a UV-3600 spectrophotometer (Shimadzu, Japan), while the dynamic spectra of catalyzed reactions were recorded on a HR4000 miniature fiber optic spectrometer (Ocean Optics, USA) with a BDS100 light source (BWTek, USA). The TEM images were acquired on a

H-600 transmission electron microscope (Hitachi, Japan) using an acceleration voltage of 75 kV. The ultrapure water was obtained from the Integral 10 water purification system (Millipore, France).

Synthesis of gold nanorods with different aspect ratios

Gold nanorods with different aspect ratios were prepared by an improved version of the well-known seeding growth method, based on the reduction of $HAuCl_4$ with ascorbic acid in the presence of aromatic additives and CTAB-coated gold nanoparticle seeds (Nikoobakht and El-Sayed 2003; Ye et al. 2012). First, the seed solution was prepared by borohydride reduction of 10 mL $HAuCl_4$ (0. 1 mM) and CTAB (0.1 M) mixed solution. 1.8 g CTAB and 0.22 g 5-bromosalicylic acid were dissolved in 50 mL warm water (about 50 ^{o}C). Then, the mixture of CTAB and 5-bromosalicylic acid were added to 50 mL of 0.001 M $HAuCl_4$ solution. A certain amount of $AgNO_3$ solution (0.004 M) was added with gentle stirring, then the solution of 0.0778 M ascorbic acid was added. The solution was gently swirling for several seconds until it became colorless. Finally, a certain amount of seed solution was injected into the growth solution and the mixture was maintained at 30 ^{o}C for 12 h. The aspect ratio of gold nanorods was controlled by tuning the added amounts of $AgNO_3$, ascorbic acid, and seed solution. The prepared gold nanorods were cleaned twice by centrifugation at 10000 rpm for 10 min, and redispersed in deionized water. The concentrations of gold nanorods with different aspect ratios were calculated according to the Lambert–Beer law. The molar extinction coefficients of gold nanorod solutions at their longitudinal LSPR wavelengths were determined by the inductively coupled plasma (ICP) measurement (Dreaden 2012; Orendorff and Murphy 2006). Given the molar extinction coefficients and the measured absorption of gold nanorod solutions, we calculated the concentrations of gold nanorods with different sizes by using the Lambert–Beer equation.

Synthesis of gold nanorods with different sizes but with the same aspect ratios

Three kinds of gold nanorods with the same aspect ratios were prepared using different methods. Gold nanorods with the longitudinal LSPR located at 696 nm were obtained by the improved seeding growth method with aromatic additives (Ye et al. 2012). Gold nanorods with the LSPR at 699 nm were prepared by the methods in the presence of sodium oleate (Ye et al. 2013), while the gold nanorods with the LSPR centered at 712 nm were synthesized by the popular seeding growth method (Nikoobakht and El-Sayed 2003).

Synthesis of gold nanorods with different sizes but with the rough volumes

Three gold nanorod samples with the rough volumes were prepared using the improved version proposed by Murray group (Ye et al. 2012). The longitudinal LSPR peaks of gold nanorods were controlled by tuning the added amounts of $AgNO_3$, ascorbic acid, and seed solution.

The catalyzed reduction of Eosin Y using gold nanorods

The catalytic reactions were carried out by mixing 1.5 mL of an aqueous solution of Eosin Y (4×10^{-5} M) with 0.5 mL of different sizes of gold nanorods in a 4-mL quartz cuvette. After several minutes of mixing, 0.5 mL of fresh $NaBH_4$ (0.12 M) was rapidly injected into the reaction mixture to start the reduction reaction. The kinetics of the reaction were investigated by recording the absorption intensities of the system at different time intervals using a fiber optic spectrometer.

Results and discussion

Preparation and characterization of gold nanorods

The seed-mediated growth method was widely used for preparing gold nanorods with different aspect ratios. However, gold nanorods with local surface plasmon resonance (LSPR) less than 700 nm were difficult to prepare, and there were a few nonrod-shaped particles in the prepared nanorod solution (Ye et al. 2012). To eliminate the interference of the nonuniformity of the as-synthesized gold nanorods to the catalysis, we chose the improved synthesis of gold nanorods using aromatic additives, as was proposed by

Murray group (Ye et al. 2012). In this method, the dimensions of gold nanorods were controlled by several ingredients or parameters, including the types of aromatic additives, and the amounts of AgNO₃, ascorbic acid, and the seed solution. In the present work, 5-bromosalicylic acid was used as the aromatic additive, and the LSPRs of gold nanorods were tuned by adding suitable amounts of AgNO₃, ascorbic acid, and seed solution. The TEM images of the prepared gold nanorods are shown in Fig. 1a–e. The obtained gold nanorods displayed good uniform in shape and size. The level of shape purities in the prepared batches was considerably higher than those of previous gold nanorods synthesized by the seed-mediated growth without adding aromatic additives, particularly when the aspect ratio was small. However, a very

small fraction of nanospheres or nanocubes existed in the as-synthesized gold nanorods, which had little effect on the catalysis.

The normalized optical absorption spectra of gold nanorods prepared by adding 5-bromosalicylic acid are shown in Fig. 1f. The absorption spectra had two absorption peaks: the transverse LSPR peak around 520 nm, and the longitudinal LSPR peak between 600 and 900 nm. The longitudinal LSPR peaks were strong and sharp, indicating that the synthesized gold nanorods had a very good purity, as was evidenced by the TEM images. Moreover, the dimensions and aspect ratios of gold nanorods were measured from TEM images, as listed in Table 1. With the increasing wavelength of the longitudinal LSPR peak, the aspect ratios of gold nanorods were enhanced. However, the lengths and

Fig. 1 TEM images of gold nanorods with varying longitudinal plasmon band: a 615 nm; b 672 nm; c 718 nm; d 753 nm; e 848 nm. f UV–Vis spectra of gold nanorods with varying longitudinal plasmon band as those in (a–e)
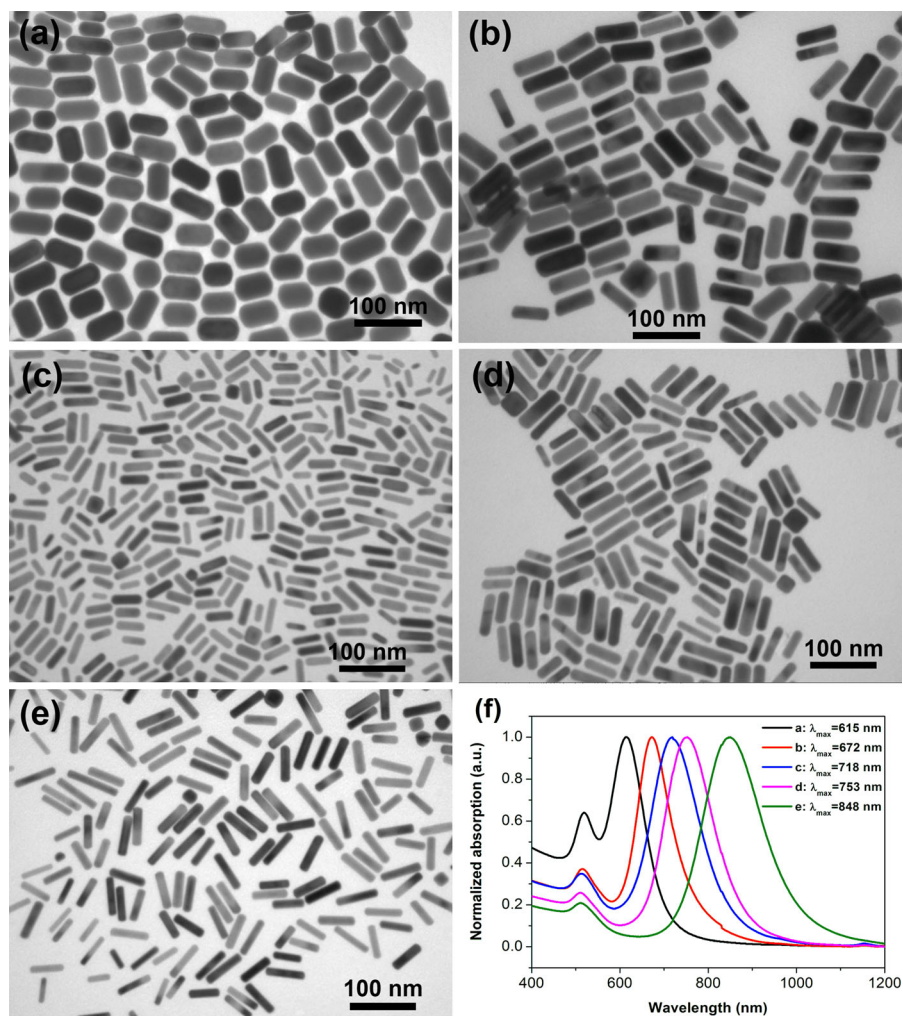
Table 1 The parameters of the prepared gold nanorods with different LSPR peaks

	λ_{max} (nm)	Length (nm)	Diameter (nm)	Aspect ratio
a 130[a]	615	59.28	32.83	1.84
b 150	672	64.01	26.33	2.43
c 150	718	39.36	13.11	3.00
d 138	753	54.50	16.94	3.22
e 135	848	55.22	13.63	4.05

[a] The number of gold nanorod used for size calculation

diameters exhibited erratic variability. Gold nanorods with medium aspect ratio had the smallest size in length and diameter, which was different from gold nanorods prepared by the silver-assisted seed-mediated growth without aromatic additives. In the latter method, the length of gold nanorods usually keeps in line with the wavelength of the longitudinal LSPR peak and aspect ratio, while there are always no significant changes in the size of diameter.

Three gold nanorod samples with different sizes but with similar aspect ratios were prepared for the investigation of the effect of aspect ratio. The TEM images and absorption intensities of the prepared gold nanorods are shown in Fig. 2. The dimensions and aspect ratios of gold nanorods were measured from TEM images, as listed in Table 2. The obtained nanorods had the similar longitudinal LSPR peaks around 705 nm, but their lengths and diameters were quite different. The calculated aspect ratios were not exactly the same as those that were expected. The reason for the slight differences in their aspect ratios was that these three gold nanorods were prepared by distinct methods. Also, another three kinds of gold nanorods with different sizes but with the rough volumes were prepared to study the effect of surface area. The TEM images and the absorption intensities of gold nanorods are shown in Fig. 3. The sizes and aspect ratios of gold nanorods were different, and the calculated volumes and surface areas are given in the Table 3. The volume of three nanorod samples is not similar as expected, however, the surface area slightly decreased with the increase of the aspect ratio. It is worth to note that the obtained gold nanorods were not perfect in length and diameter as the request in theory.

Production of radicals in catalyzed reduction of Eosin Y

In our previous research, we found that the reduction pathway of EY changed from two-electron to one

electron when gold solid or hollow nanosphere were used as catalysts (Mahmoud and Weng 2013; Weng et al. 2012). In the present work, gold nanorods were employed as the nanocatalysts to catalyze the reduction of EY and the pathway was the same as those used for gold solid and hollow nanosphere catalysts, as shown in Fig. 4a. In the presence of gold nanorods, EY was reduced through the one-electron reduction, and the bi-anionic form (EY^{2-}) of EY received one electron from borohydride (BH_4^-), forming a semi-quinone intermediate (EY^{3-}).

We recorded the time-dependent absorption spectrum of reduction reaction of EY using BH_4^- in the presence of gold nanorods with different aspect ratios. Figure 4b shows the typical results of reduction reactions catalyzed by gold nanorods with the longitudinal LSPR peak located at 718 nm (set C). As shown in Fig. 4b, the bi-anionic form (EY^{2-}) of EY had a strong absorption peak at 516 nm (Goux et al. 2007; Zhang et al. 2011), and the intensity of EY^{2-} decreases slowly over time during the first few seconds owing to the formation of EY^{4-}. Then the intensity of EY^{2-} declined at a rapid rate, and at the same time, a new absorption peak appeared at 405 nm. The new peak at 405 nm corresponds to the radical of EY (noted EY^{3-} in Fig. 4a), resulting from one-electron reduction of EY (Goux et al. 2007; Weng et al. 2012; Zhang et al. 2011). However, as the time increases, the intensity of EY^{3-} increases first and then decreases because of EY^{3-} converting to EY^{4-}.

Plotting the intensity of peaks at 516 and 405 nm versus time, the complete time-dependent absorption of EY^{3-} and EY^{2-} in the presence of five groups of nanorods were obtained, as shown in Fig. 5a. The process of catalyzed reduction of EY had three different stages, according the intensities change of EY^{3-} and EY^{2-}. At the first stage, the intensity of EY^{2-} increased rapidly after the addition of BH_4^-, then the intensity slightly decreased. The sudden increase of intensity at 516 nm attributed to the

Fig. 2 TEM images of gold nanorods with similar aspect ratios: **a** 696 nm; **b** 699 nm; **c** 712 nm; **d** UV–Vis spectra of gold nanorods with similar aspect ratios to those in (**a–c**)
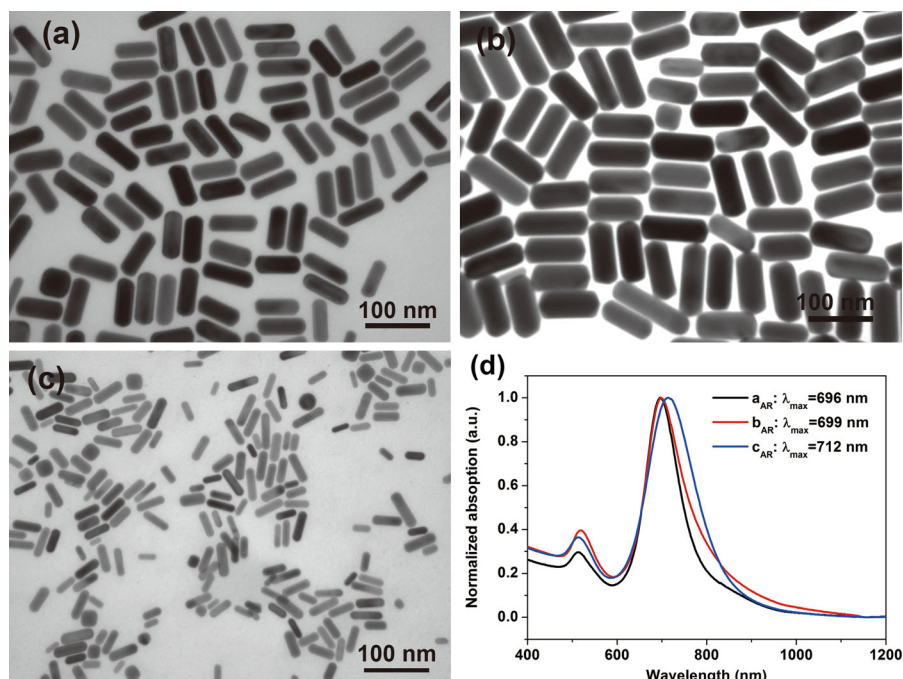
Table 2 The parameters of the prepared gold nanorods with similar aspect ratios

	λ_{max} (nm)	Length (nm)	Diameter (nm)	Aspect ratio
a 127[a]	696	70.56	25.62	2.75
b 117	699	95.17	38.37	2.48
c 151	712	38.16	13.57	2.81

[a] The number of gold nanorod used for size calculation

improvement of hydrolysis of EY. The enhancement of hydrolysis came from the increase of pH value after adding the BH_4^- (Mahmoud and Weng 2013; Weng et al. 2012). The intensity of EY^{2-} then slightly decreased was due to the reduction of EY^{2-} though the two-electron pathway, and EY^{2-} partly changed to EY^{4-}. As the time scale of the first stage was different with varied sets of gold nanorods, the remained quantity of EY^{2-} was different at the end of the stage one, as shown in Fig. 5b. So, it would happen that gold nanorods with longer stage one had more EY^{2-} reduced to EY^{4-} before the appearance of EY^{3-}. However, the speeds of EY^{2-} reduced to EY^{4-} with different sets of gold nanorods were slow and similar, and the intensities of EY^{2-} (516 nm) were around 1.2 at the end of stage one except group C, as shown in Fig. 5b (red curve). For group C, the time of the stage

one was about 60 s, there were almost no EY^{2-} reduced to EY^{4-}, so the intensity of 516 nm was higher than that of other groups. In addition, we thought the time scale was also dependent on the shape and size of gold nanorods, which was in agreement with our previous work (Weng et al. 2012). The time scale of the stage one may partially indicated the activity of gold nanorods. The shorter the time scale of the stage one was, the more active the gold nanorods were. Thus, the decreased quantity of EY^{2-} due to reducing to EY^{4-} at the first stage had no obvious influence on the production of the radicals EY^{3-} and the evaluation of catalytic effect of gold nanorods.

The second stage started when the intensity of EY^{2-} was suddenly decreased. Meanwhile, a new peak at 405 nm began to appear and its intensity reached the summit. At this stage, EY^{2-} was reduced

Fig. 3 TEM images of gold nanorods with rough volumes: **a** 745 nm; **b** 814 nm; **c** 923 nm; **d** UV–Vis spectra of gold nanorods with rough volumes as that in (**a–c**)
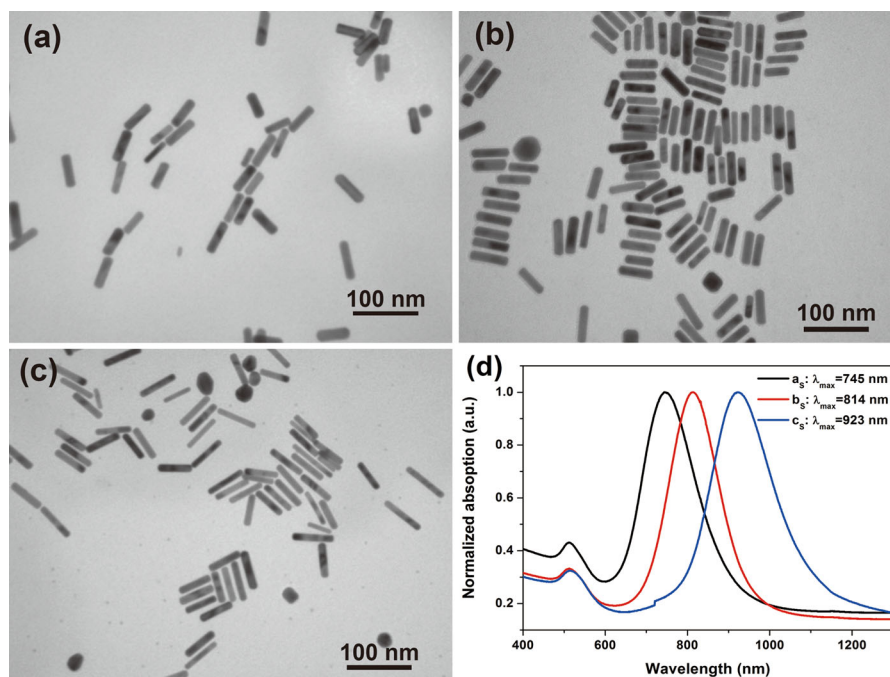
Table 3 The parameters of the prepared gold nanorods with rough volumes

|	$\lambda_{\max}$ (nm)	Length (nm)	Diameter (nm)	Aspect ratio	Volume (nm^3)	Surface area (nm^2)
a 95[a]	745	45.11	14.02	3.22	6960.47	2294.47
b 108	814	50.07	12.85	3.90	6490.13	2279.51
c 102	923	53.60	11.06	4.85	5146.89	2053.48

[a] The number of gold nanorod used for size calculation

though one-electron pathway and transferred to the radical EY^{3-}. The third stage began when the rate of the disappearance of EY^{2-} decreased and the intensity of EY^{3-} started to decline. At the third stage, the radical EY^{3-} was thought to be reduced to a new green dye with a long enough time (Mahmoud and Weng 2013), and the decrease of intensity at 516 nm has a rate close to that of the first stage, indicating the EY^{2-} was reduced again by accepting two electrons.

As above stated, the catalyzed reduction of EY using gold nanorods was similar to that using gold nanospheres (solid and hollow) (Weng et al. 2012). However, the time of the first stage was shorter when using gold nanorods as catalysts. As we all know, the catalytic effect of nanocatalysts is dependent on the shape and composition (Ahmadi et al. 1996; Zeng et al. 2010). Besides the effect of shape and

composition, the concentration of nanocatalysts also plays an important role in the catalysis. For the same type for gold nanoparticles, the time of the first stage decreased as the concentrations of gold nanoparticles increased (Weng et al. 2012). In the present work, the concentration of gold nanorods was 0.15 nM, which much exceeded that of gold solid or hollow nanospheres (pM level) (Weng et al. 2012). So, the time of the first stage was shorter than that of using gold nanospheres.

### Gold nanorods with the smallest size being the most efficient

The reduction of EY^{2-} by BH_4^- in the presence of gold nanoparticles leads to the formation of a mixture of EY^{3-} and EY^{4-}. At the first and third stages, the
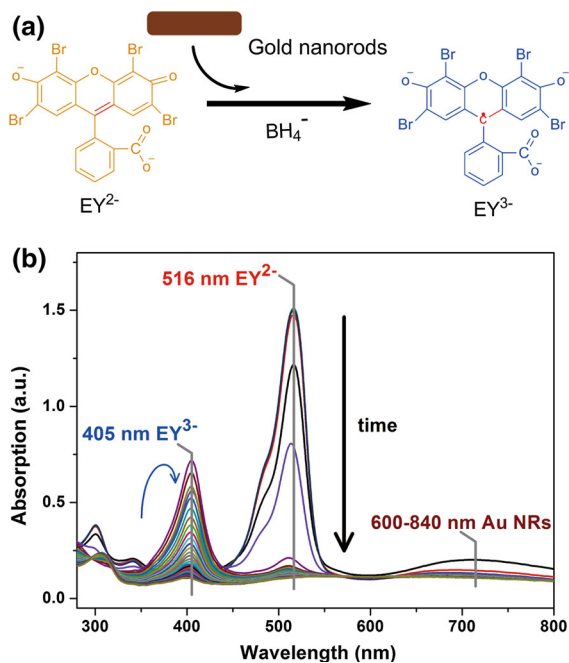
Fig. 4 The catalytic processes for EY to EY^{3-} and EY^{4-}: **a** Scheme of the one-electron reduction of EY; **b** UV–Vis spectra of EY during reduction catalyzed with gold nanorods

rate constants of transformation of EY^{2-} to EY^{4-} were nearly the same, regardless of the shape and concentration of gold nanocatalysts. However, at the second stage, the rate constant and lifetime of transformation from EY^{2-} to EY^{3-} were different for varied nanocatalysts—especially the intensities of the radical EY^{3-} also were different between hollow and solid gold nanospheres (Weng et al. 2012). The differences in the transformations of EY^{2-} to EY^{3-} make it possible to evaluate the efficiency of each set of gold nanorods.

To investigate the size on the catalytic effect of gold nanorods, we calculated the production of the radical EY^{3-} in the presence of each set of gold nanorods, as shown in Fig. 6. To ensure a quantitative comparison between gold nanorods with different aspect ratios, the concentration of gold nanorods (0.15 nM) had been kept constant for all the tested reactions. With the increasing aspect ratios of gold nanorods, the production trend of the radical EY^{3-} showed no consistency. It seemed that there was no obvious correlation between the aspect ratios of the gold nanorods and the production for the reduction of EY^{2-} to EY^{3-}. However, gold nanorods with the smallest sizes (set C) had the highest production of EY^{3-}, which was about
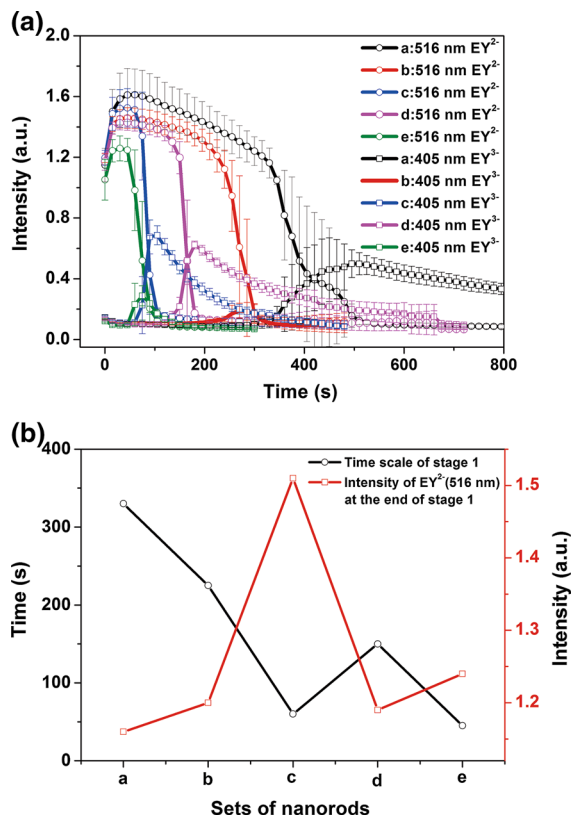
Fig. 5 **a** The complete time-dependent absorption intensities of EY^{2-} and EY^{3-}. **b** Time scale of the stage one and the intensities of EY^{2-} at the end of stage one for five groups of nanorods. (Color figure online)
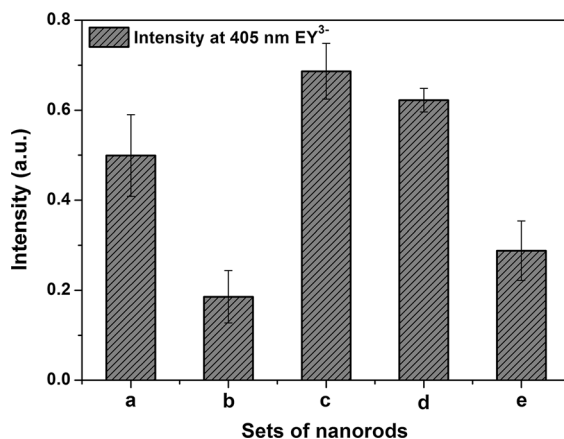
**Fig. 6** The production of EY^{3-} for different sets of gold nanorods

3.5 times higher than the least-active nanorods (set B). Furthermore, the set C gold nanorods had the moderate values of aspect ratios in five sets of nanorods. To the

best of our knowledge, it was observed for the first time that gold nanorods with intermediate aspect ratio (3.00) showed the highest activity during the reduction reaction of EY^{2-} to EY^{3-}.

As is well known, gold nanorods with the same aspect ratios may have different sizes. To investigate the influence of aspect ratio on the catalytic effect of gold nanorods, we used the nanorods with the similar aspect ratios but with different sizes to catalyze the reduction of EY. The three kinds of gold nanorods bears nearly the same aspect ratio, but the corresponding yields of the radicals of EY^{3-} are different, as shown in Fig. 7. Gold nanorods with smallest dimensions of length and diameter produced the highest intensity of EY^{3-}, which is in agreement with the results of gold nanorods with different aspect ratios. The results further indicated that the size was the primary factor in determining the catalytic effect of gold nanorods.

Gold nanorods with the smallest size were the most efficient for the catalyzed reduction from EY^{2-} to EY^{3-}, which is in accordance with the catalyzed p-nitrophenol reduction and CO oxidation by supported gold nanoparticles (Haruta et al. 1989; Panigrahi et al. 2007). Some researchers have already focused on the effect of size of nanoparticles in catalyzed reaction (Fenger et al. 2012; Zhou et al. 2009). Most of the reports found that the nanocatalysts with smaller size usually have the higher activity. Smaller nanocatalysts are more active because they have a larger number of coordinatively unsaturated surface atoms (Panigrahi et al. 2007). The ratio of
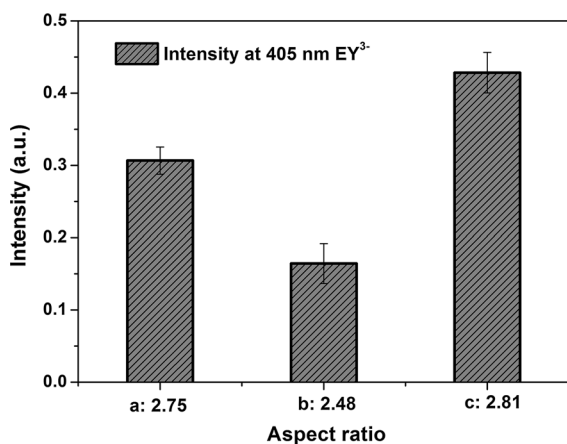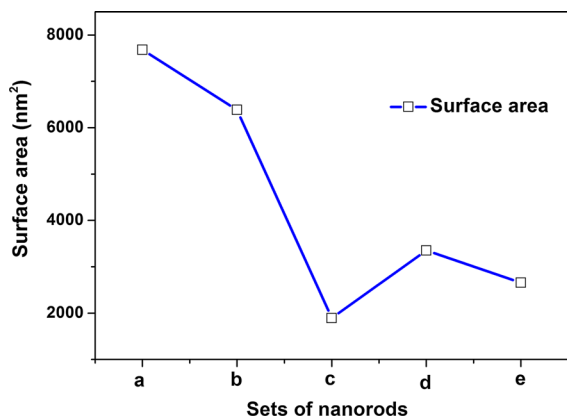

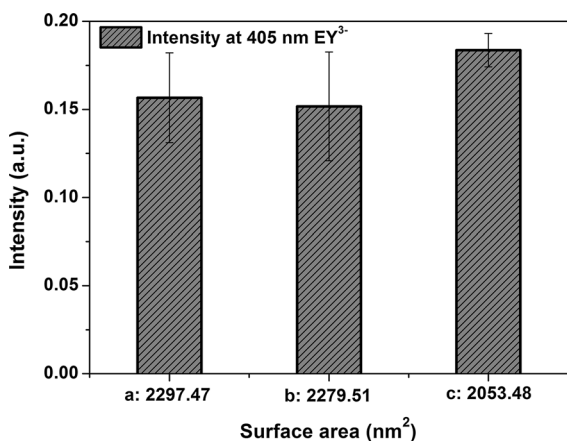**Fig. 7** The production of EY^{3-} for gold nanorods with similar aspect ratios

coordinatively unsaturated surface atoms in small-sized catalysts is higher than that in big-sized nanoparticles. In the present work, the gold nanorods of set C had the smallest size (length and diameter), so the highest production of EY^{3-} achieved during the reduction of EY^{2-} was observed due to the higher ratio of coordinatively unsaturated surface atoms.

For the gold nanorods of set A, their size remained in the fourth position (in terms of length), while the production of EY^{3-} remained in the third position. It indicated that the correlation between the size and the catalytic activity of gold nanorods was not strong. This may be related with the configuration of EY^{2-} being absorbed onto the surface of gold nanorods. The surface charges of the prepared gold nanorods are positive, and EY^{2-} is a bi-anion. The groups with negative charge (–OH and –COOH) distribute in the two sides of EY^{2-}, which leads to a "flat lying" configuration for EY^{2-} absorption onto the surface of gold nanorods though the electrostatic interactions. The configuration of "flat lying" requires a larger surface area for adsorption. Thus, the surface areas of gold nanorods may play a role that cannot be ignored in the catalyzed reaction. The surface areas of the prepared gold nanorods were calculated according to the previous report, and are shown in Fig. 8. The gold nanorods of set A had the maximum value of the surface area, which implied that set A could load the highest amount of EY^{2-} on their surface. Therefore, the production of EY^{3-} was enhanced to a certain extent.

To check the effect of the surface area on the catalytic activity of gold nanorods, we prepared three gold nanorod groups with the similar rough volumes but with different aspect ratios. The yields of the radicals EY^{3-} catalyzed by three kinds of gold nanorods had no obvious relationship with the surface areas, as shown in Fig. 9. Gold nanorods with the minimum surface area produced the highest yield of EY^{3-}, which was inconsistent with the expected results. The possible reasons are as follows: (1) the differences in the surface areas of employed gold nanorods were not remarkable, thus having no effect on the production of EY^{3-}; (2) the major factor influencing the catalytic effect was the size of gold nanorods, which was proven by the results of gold nanorods with the smallest surface areas (Group C in Fig. 9). The effect of surface area would materialize when the difference was sufficiently large, as per the

Fig. 8 The calculated surface areas of different sets of gold nanorods

Fig. 9 The production of EY^{3-} for gold nanorods with different surface areas

results shown in the first group of nanorods. However, we presumed that the surface area still played the minor role in the catalytic effect and then caused the weak correlation between the size and the catalytic activity of gold nanorods.

Conclusions

In summary, we have demonstrated that gold nanorods have the catalytic effects similar to gold nanospheres in the catalyzed reduction of Eosin Y. The production of radical EY^{3-} induced by gold nanocatalysts is dependent on the size of gold nanorods, and the smallest nanorods have the highest yield of EY^{3-}. The

higher production of EY^{3-} catalyzed by small-sized nanorods is attributed to the fact that small nanorods have a larger number of coordinatively unsaturated surface atoms available for catalysis. In addition, the amount of absorbed molecules on the surface of nanocatalysts also has a minor effect on the conversion efficiency of EY^{2-} to EY^{3-} for gold nanocatalysts.

References

Ahmadi TS, Wang ZL, Green TC, Henglein A, El-Sayed MA (1996) Shape-controlled synthesis of colloidal platinum nanoparticles. Science 272:1924–1926. doi:10.1126/science.272.5270.1924

Arvizo R, Bhattacharya R, Mukherjee P (2010) Gold nanoparticles: opportunities and challenges in nanomedicine. Expert Opin Drug Deliv 7:753–763. doi:10.1517/17425241003777010

Bannerjee NR, Negi AS (1973) Polarograms of eosin (2,4,5,7-tetrabromo-(R)-fluorescein) in aqueous buffers. Electrochim Acta 18:335–342. doi:10.1016/0013-4686(73)85001-7

Dreaden EC (2012) Chemistry, photophysics, and biomedical applications of gold nanotechnologies. Georgia Institute of Technology, Atlanta

Dreaden EC, Alkilany AM, Huang XH, Murphy CJ, El-Sayed MA (2012) The golden age: gold nanoparticles for biomedicine. Chem Soc Rev 41:2740–2779. doi:10.1039/C1CS15237H

Dreaden EC, Mackey MA, Huang X, Kang B, El-Sayed MA (2011) Beating cancer in multiple ways using nanogold. Chem Soc Rev 40:3391–3404. doi:10.1039/C0CS00180E

Fenger R, Fertitta E, Kirmse H, Thunemann AF, Rademann K (2012) Size dependent catalysis with CTAB-stabilized gold nanoparticles. Phys Chem Chem Phys 14:9343–9349. doi:10.1039/C2CP40792B

Ghosh P, Han G, De M, Kim CK, Rotello VM (2008) Gold nanoparticles in delivery applications. Adv Drug Delivery Rev 60:1307–1315. doi:10.1016/j.addr.2008.03.016

Giljohann DA, Seferos DS, Daniel WL, Massich MD, Patel PC, Mirkin CA (2010) Gold nanoparticles for biology and medicine. Angew Chem Int Ed 49:3280–3294. doi:10.1002/anie.200904359

Goux A, Pauporté T, Lincot D, Dunsch L (2007) In situ ESR and UV/Vis spectroelectrochemical study of Eosin Y upon reduction with and without Zn(II) Ions. ChemPhysChem 8:926–931. doi:10.1002/cphc.200700009

Han G, Ghosh P, Rotello VM (2007) Functionalized gold nanoparticles for drug delivery. Nanomedicine 2:113–123. doi:10.2217/17435889.2.1.113

Haruta M, Yamada N, Kobayashi T, Iijima S (1989) Gold catalysts prepared by coprecipitation for low-temperature oxidation of hydrogen and of carbon monoxide. J Catal 115:301–309. doi:10.1016/0021-9517(89)90034-1

Hutchings GJ (2005) Catalysis by gold. Catal Today 100:55–61. doi:10.1016/j.cattod.2004.12.016

Issa IM, Issa RM, Ghoneim MM, Temerk YM (1973) Polarography of eosin and erythrosin in solutions of varying pH at the DME. Electrochim Acta 18:265–270. doi:10.1016/0013-4686(73)80024-6

Kundu S, Lau S, Liang H (2009) Shape-controlled catalysis by cetyltrimethylammonium bromide terminated gold nanospheres, nanorods, and nanoprisms. J Phys Chem C 113:5150–5156. doi:10.1021/jp811331z

Li Y, Liu Q, Shen W (2011) Morphology-dependent nanocatalysis: metal particles. Dalton Trans 40:5811–5826. doi:10.1039/C0DT01404D

Lin F, Wise G (2009) Detection of proteins and sialoglycoproteins in polyacrylamide gels using eosin Y stain. In: Walker J (ed) The protein protocols handbook. Springer protocols handbooks. Humana Press, New York, pp 575–578. doi:10.1007/978-1-59745-198-7_53

Mahmoud MA, El-Sayed MA (2011) Time dependence and signs of the shift of the surface plasmon resonance frequency in nanocages elucidate the nanocatalysis mechanism in hollow nanoparticles. Nano Lett 11:946–953. doi:10.1021/nl103265s

Mahmoud MA, Weng GJ (2013) Nanocatalysis production of photoactive radicals. Catal Commun 38:63–66. doi:10.1016/j.catcom.2013.04.021

Mahmoud MA, Narayanan R, El-Sayed MA (2013) Enhancing colloidal metallic nanocatalysis: sharp edges and corners for solid nanoparticles and cage effect for hollow ones. Acc Chem Res. doi:10.1021/ar3002359

Mali SS, Betty CA, Bhosale PN, Patil PS (2012) Eosin-Y and N3-Dye sensitized solar cells (DSSCs) based on novel nanocoral TiO₂: a comparative study. Electrochim Acta 59:113–120. doi:10.1016/j.electacta.2011.10.043

Nikoobakht B, El-Sayed MA (2003) Preparation and growth mechanism of gold nanorods (NRs) using seed-mediated growth method. Chem Mater 15:1957–1962. doi:10.1021/cm020732l

Orendorff CJ, Murphy CJ (2006) Quantitation of metal content in the silver-assisted growth of gold nanorods. J Phys Chem B 110:3990–3994. doi:10.1021/jp0570972

Panigrahi S et al (2007) Synthesis and size-selective catalysis by supported gold nanoparticles: study on heterogeneous and homogeneous catalytic process. J Phys Chem C 111:4596–4605. doi:10.1021/jp067554u

Saha K, Agasti SS, Kim C, Li X, Rotello VM (2012) Gold nanoparticles in chemical and biological sensing. Chem Rev 112:2739–2779. doi:10.1021/cr2001178

Sardar R, Funston AM, Mulvaney P, Murray RW (2009) Gold nanoparticles: past, present, and future. Langmuir 25:13840–13851. doi:10.1021/la9019475

Sau TK, Pal A, Pal T (2001) Size regime dependent catalysis by gold nanoparticles for the reduction of Eosin. J Phys Chem B 105:9266–9272. doi:10.1021/jp011420t

Sharma P, Brown S, Walter G, Santra S, Moudgil B (2006) Nanoparticles for bioimaging. Adv Colloid Interface Sci 123–126:471–485. doi:10.1016/j.cis.2006.05.026

Sperling RA, Rivera gil P, Zhang F, Zanella M, Parak WJ (2008) Biological applications of gold nanoparticles. Chem Soc Rev 37:1896–1908. doi:10.1039/B712170a

Srivastava S, Sharma SK, Sharma RK (2011) Synthesis of gold nanorods using concentrated aerosol OT in hexane and its application as catalyst for the reduction of eosin. Colloids Surf A 373:61–65. doi:10.1016/j.colsurfa.2010.10.022

Thompson DT (2007) Using gold nanoparticles for catalysis. Nano Today 2:40–43. doi:10.1016/s1748-0132(07)70116-0

Weng GJ, Mahmoud MA, El-Sayed MA (2012) Nanocatalysts can change the number of electrons involved in oxidation–reduction reaction with the nanocages being the most efficient. J Phys Chem C 116:24171–24176. doi:10.1021/jp308869m

Wilson R (2008) The use of gold nanoparticles in diagnostics and detection. Chem Soc Rev 37:2028–2045. doi:10.1039/B712179m

Xia L, Zhao H, Liu G, Hu X, Liu Y, Li J, Yang D (2011) Degradation of dyes using hollow copper microspheres as catalyst. Colloids Surf A 384:358–362. doi:10.1016/j.colsurfa.2011.04.016

Ye X, Jin L, Caglayan H, Chen J, Xing G, Zheng C, Doan-Nguyen V, Kang Y, Engheta N, Kagan CR, Murray CB (2012) Improved size-tunable synthesis of monodisperse gold nanorods through the use of aromatic additives. ACS Nano 6:2804–2817. doi:10.1021/nn300315j

Ye X, Zheng C, Chen J, Gao Y, Murray CB (2013) Using binary surfactant mixtures to simultaneously improve the dimensional tunability and monodispersity in the seeded growth of gold nanorods. Nano Lett 13:765–771. doi:10.1021/nl304478h

Yoshida T et al (2009) Electrodeposition of inorganic/organic hybrid thin films. Adv Funct Mater 19:17–43. doi:10.1002/adfm.200700188

Zeng J, Zhang Q, Chen JY, Xia YN (2010) A comparison study of the catalytic properties of Au-based nanocages, nanoboxes, and nanoparticles. Nano Lett 10:30–35. doi:10.1021/nl903062e

Zhang JB, Sun LN, Yoshida T (2011) Spectroelectrochemical studies on redox reactions of eosin Y and its polymerization with Zn²⁺ ions. J Electroanal Chem 662:384–395. doi:10.1016/j.jelechem.2011.09.008

Zhou X, Xu W, Liu G, Panda D, Chen P (2009) Size-dependent catalytic activity and dynamics of gold nanoparticles at the single-molecule level. J Am Chem Soc 132:138–146. doi:10.1021/ja904307n

Zhu Y, Qian H, Das A, Jin R (2011) Comparison of the catalytic properties of 25-atom gold nanospheres and nanorods. Chin J Catal 32:1149–1155. doi:10.1016/S1872-2067(10)60238-0